Revista Brasileira de Engenharia Biomédica,
v. 23, n. 3, p. 263-275, dezembro 2007

ISSN 1517-3151

Artigo Original
Recebido em 30/07/2007, aceito em 30/12/2007

Improvement of gas exchange measurements in ergospirometry with the use of optimal filters for O_2 and CO_2 transducers

Aprimoramento de medição de trocas gasosas em ergoespirometria com o uso de filtros ótimos para transdutores de O_2 e CO_2

Marcelo Alexandre Garcia
Laboratório de Engenharia Biomédica,
Escola Politécnica / USP

Vítor Heloiz Nascimento
Laboratório de Processamento de Sinais,
Escola Politécnica / USP

José Carlos Teixeira de Barros Moraes*
Laboratório de Engenharia Biomédica,
Escola Politécnica / USP
Av. Prof. Luciano Gualberto, trav. 3, n. 158, sl. D2-05,
05508-900 São Paulo, SP
E-mail: jcmoraes@leb.usp.br

*Corresponding author

Abstract
The improvement of human gas exchange measurement accuracy in breath-by-breath analysis requires a suitable compensation method for the narrow passband of the gas transducers used. Despite the fact that the design of optimal filters for these transducers requires techniques such as Wiener filtering or recursive least squares approximation, these techniques have not yet been applied to ergospirometry transducers. In this paper we propose a method for designing digital filters for such transducers with application in ergospirometry. The designed filters were applied to signals acquired with infrared carbon dioxide transducers, electrochemical oxygen transducers and a paramagnetic oxygen transducer. Two techniques were successfully evaluated: a modified normalized least-mean square (NLMS) adaptive algorithm and a modified FFT-Wiener filtering. The optimal filters were designed with least mean-square error criteria. The average power spectral densities of oxygen and carbon dioxide concentration signals were used in the computation of the optimal filters. Filter performance was evaluated with a breathing simulator mechanism with controlled oxygen and carbon dioxide exchange rates. Gas exchange measurements obtained with and without the optimal filters were compared to the values predicted for the simulator setup. Results have shown that the optimal filters can reduce the average gas exchange underestimation by up to 8 times. The increase of measurement error with an increase of respiratory rate was also reduced by up to 65%.

Keywords: Ergospirometry, Dynamic response compensation, Adaptive filtering, FFT-Wiener filtering, Breath-by-breath analysis.

Resumo
O aperfeiçoamento da acurácia em medições de trocas gasosas respiração-a-respiração em seres humanos requer um método adequado de compensação da estreita banda de passagem dos transdutores de gás utilizados. Apesar de um projeto de filtros ótimos para estes transdutores requerer técnicas como filtragem de Wiener ou aproximações recursivas por mínimos quadrados, estas técnicas ainda não têm sido aplicadas em transdutores para ergoespirometria. Neste trabalho é proposto um método para projetos de filtros digitais para tais transdutores com aplicação em ergoespirometria. Os filtros obtidos foram aplicados em sinais adquiridos com transdutores de dióxido de carbono, transdutores de oxigênio eletroquímicos e um transdutor de oxigênio paramagnético. Duas técnicas foram avaliadas com sucesso: um algoritmo adaptativo NLMS modificado e um filtro FFT-Wiener modificado. Os filtros ótimos foram projetados utilizando o critério de mínimo erro quadrático médio. A densidade espectral de potência média dos sinais de concentrações de oxigênio e dióxido de carbono foi considerada no cálculo dos filtros ótimos. O desempenho dos filtros foi avaliado com um mecanismo simulador de respiração com as trocas gasosas controladas. As medidas de trocas gasosas obtidas com e sem os filtros ótimos foram comparadas com os valores preditos pelo simulador. Os resultados mostraram que os filtros ótimos podem reduzir em até 8 vezes a subestimação média nas medições das trocas gasosas. A tendência de aumento do erro de medição com o aumento da freqüência respiratória também foi reduzida em até 65%.

Palavras-chave: *Ergoespirometria, Compensação de resposta dinâmica, Filtros adaptativos, Filtros FFT-Wiener, Análise respiração-a-respiração.*

Introduction

The measurement of energy expenditure in the human body can be performed by indirect calorimetry based on the relation between the patient's airway gas exchange (O_2 consumption and CO_2 production) and the metabolism of nutrients (Macfarlane, 2001; McArdle *et al.*, 1996; Weisman and Zeballos, 2001). Researchers have used energy expenditure measurement equipment such as ergospirometers to evaluate physical and respiratory abilities in patients under respiratory or cardiovascular care and in athletes. For further information about the topic, one can refer to ATS/ACCP (2003), Lear *et al*. (1999), Madama (1993), Myers and Madhavan (2001), Singh (2001), White and Evans (2001) and Zeballos and Weisman (1994).

However, the accuracy of this kind of equipment should not be influenced by parameters such as respiratory flow wave shape and respiratory rate. An ergospirometer can perform accurate breath-by-breath gas exchange measurements only if it uses a suitable compensation method for the narrow passband of the gas transducers.

Previous studies have demonstrated that the accuracy of gas exchange measurements in breath-by-breath analysis can be significantly improved by the enhancement of the transducer signals. Different techniques have been tested for enhancement of CO_2 and O_2 concentration measurements: first-order compensation (Nogushi *et al.*, 1982), second order compensation (Arieli and Van Liew, 1981; Bates *et al.*, 1983; Wong *et al.*, 1998), third-order compensation (Turner and Culbert, 1993), inverse filtering or deconvolution filtering (Farmery and Hahn, 2000; Shykoff and Swanson, 1987), Wiener filtering (Bates *et al.*; 1983; Garcia *et al.*, 2002) and adaptive filtering (Garcia *et al.*, 2002).

Also, Wiener filter design and even adaptive techniques must consider the power spectral density (PSD) of the true input signal for the calculation of the optimal enhancement filter, which was first evaluated by Garcia *et al.* (2007) for subjects under ergospirometric testing. In that work, Garcia *et al.* obtained samples of human respiratory flow, O_2 concentration and CO_2 concentration signals from 20 healthy subjects and evaluated the average power spectral density (PSD) of these signals in four progressive levels of exercise in a cycle ergometer. Auto regressive moving average models were designed to represent the PSD of each phase and the mean PSD of all phases. Those PSD curves were used as input signal PSD to design the present NLMS-adaptive filters and Wiener filters.

The improvement of response time in infrared CO_2 transducers and electrochemical O_2 transducers in the last decades made this type of transducer suitable for breath-by-breath analysis. Modern ergospirometers no longer need a mass spectrometer for fast measurement of gas concentrations. We noticed that all studies before 2002 evaluated the dynamic response of mass spectrometers, which nowadays are not commonly used in commercial ergospirometry equipment. Despite the fact that the design of optimal filters demands techniques such as Wiener filters or recursive least squares approximation, these techniques have not been yet described for application in ergospirometry without the use of a mass spectrometer.

In this paper we evaluate five state-of-the art transducers for ergospirometry purposes: two O_2 galvanic cell transducers, one O_2 paramagnetic transducer and two CO_2 infrared absorption transducers, and compare their performance in terms of gas exchange mean error of the optimal filter obtained with adaptive filtering (Diniz, 1997; Sayed, 2003) and the FFT-Wiener technique (Press, 1992). Both filters were designed using the average PSD of respiratory human signals previously evaluated by Garcia *et al.* The use of these filters provided better results than simple inverse filtering because the signal-to-noise ratio (SNR) in the transducers is very small at higher frequencies, which can result in undesirable amplification of background noise (Garcia *et al.*, 2002).

The goal of this work is to develop a method for designing optimal filters for O_2 and CO_2 transducers, which compensate as much as possible for their small bandwidth. To reach this goal, we developed mathematical models for those transducers which represent their dynamic response and background noise. We validate our results with the simulation of human breath in a mechanical system with known O_2 intake ($\dot{V}O_2$) and CO_2 expenditure ($\dot{V}CO_2$) and the comparison of errors in gas exchange measurements with and without the optimal filters.

Methods

Investigated transducers

This research evaluated the dynamic response and calculated optimal filters for the following transducers: paramagnetic O_2 transducer (Servomex, PM1111-E) with fast-response tubing configuration (sample line flow: 200 mL/min); galvanic cell O_2 transducer (Servomex, Zr733) with control board 700912 (sample line flow: 300 mL/min); O_2 analyzer

(AEI Technologies, S-3A/I) with N-22M sensor (sample line flow: 300 mL/min); infrared CO_2 transducer (Servomex, Ir1507) (sample line flow: 200 mL/min); and infrared CO_2 analyzer (AEI Technologies, CD-3A) with sensor P-61B set to fast response mode (sample line flow: 300 mL/min). The used sample line was 2.4 m long and its internal diameter was 1.15 mm.

Transducer modeling

We estimated the frequency response and the background noise of each transducer to create a Box-Jenkins model (Box and Jenkins, 1976) represented in the z-domain by the linear equation:

$$X(z) = \frac{B(z)}{F(z)} \cdot Y(z) + \frac{C(z)}{D(z)} \cdot E(z) \quad (1)$$

where $y(n) = Z^{-1}\{Y(z)\}$ is the stimulus at the transducer input (Z^{-1} denotes the inverse Z-transform and n is the sample index); $x(n) = Z^{-1}\{X(z)\}$ is the signal obtained at the output; $B(z)/F(z)$ represents an auto-regressive moving average (AR-MA) (Ljung, 1999) model for the transducer dynamic response; $C(z)/D(z)$ represents an AR-MA model for the background output noise of the transducer; and $e(n) = Z^{-1}\{E(z)\}$ is a normalized white noise signal.

The transducer output $x(n)$ can be written in the discrete time domain as a sum of a noiseless term $s(n)$ and the noise $r(n)$:

$$x(n) = s(n) + r(n) \quad (2)$$

The noiseless transducer output $s(n)$ and the background noise $r(n)$ can be calculated using the following equations:

$$\begin{aligned} s(n) = [&b_0 \cdot y(n) + b_1 \cdot y(n-1) + \cdots + b_{ob} \cdot y(n-ob) \\ &- f_1 \cdot s(n-1) - \cdots - f_{of} \cdot s(n-of)] / f_0 \end{aligned} \quad (3)$$

$$\begin{aligned} r(n) = [&c_0 \cdot e(n) + c_1 \cdot e(n-1) + \cdots + c_{oc} \cdot e(n-oc) \\ &- d_1 \cdot r(n-1) - \cdots - d_{od} \cdot r(n-od)] / d_0 \end{aligned} \quad (4)$$

where: $y(n)$ is the current transducer input sample; $e(n)$ is the current normalized white noise sample; $y(n–1)$, $y(n–2)$, etc. are past samples of $y(n)$ (the same for the other variables); b_i, f_i, c_i and d_i are coefficients of model polynomials B, F, C and D respectively; "ob", "of", "oc" and "od" are the degrees of each polynomial.

The AR-MA models B/F and C/D can be expressed by its zeroes and poles in z plane, as shown in (5) and (6):

$$\frac{B(z)}{F(z)} = k_{bf} \cdot \frac{(z - zb_1) \cdot (z - zb_2) \cdot \cdots \cdot (z - zc_{ob})}{(z - pf_1) \cdot (z - pf_2) \cdot \cdots \cdot (z - pf_{of})} \quad (5)$$

$$\frac{C(z)}{D(z)} = k_{cd} \cdot \frac{(z - zc_1) \cdot (z - zc_2) \cdot \cdots \cdot (z - zc_{oc})}{(z - pd_1) \cdot (z - pd_2) \cdot \cdots \cdot (z - pd_{od})} \quad (6)$$

where: zb_i, pf_i, zc_i and pd_i, are the zeroes and poles of the transfer functions B/F and C/D; and k_{bf} and k_{cd} are the constant gains, respectively.

Using a sampling rate of 100 Hz, B/F models for the O_2 and CO_2 transducers were obtained from their step response. Such sampling rate was chosen based on the O_2 and CO_2 gas concentration power spectral densities, both presenting no significant spectral power above 10 Hz (Garcia *et al.*, 2007). The step stimulus was generated through the rupture of a balloon inside a chamber. The balloon is filled with a gas mixture with 16% of O_2 and 4% of CO_2, in such way as to fit almost the total volume of space inside the chamber, in order to guarantee the step shape of the generated stimulus. This procedure was described in detail by Nogushi *et al*. (1982). Eight empirical step responses were averaged in order to reduce the inevitable measurement noise present when obtaining the step signal (notice that further on we will estimate the power spectrum of the noise, through polynomials $C(z)$ and $D(z)$). Before averaging, the acquired signals were synchronized with the instant of balloon rupture in order to avoid any distortion of the step response wave shape. System identification was performed with the least squares method (Ljung, 1999). The routine used is shown in Appendix A.

C/D models were obtained from the transducer signal acquisition with constant gas concentration in its input. The concentration used was the ambient concentration to minimize the influence of a possible non-linearity of the transducer background noise when the concentration in gas sample is too far from the range of concentrations in the human airway (typically 0-10% of CO_2 and 11-21% of O_2) (Nogushi *et al.*, 1982). The resulting signal had only a noise component added to a constant component. The constant component of this signal was cancelled, resulting in a time series corresponding to the transducer background noise. This data was used to estimate the coefficients of the disturbance model *C/D* separately. The coefficients of the disturbance model (*C/D*) were obtained with the least squares method (Ljung, 1999). The employed routine is shown in Appendix B. The reason for modeling the transducer background noise separately is that the step response averaging procedure described in the previous paragraph results in an averaged step with reduced noise in relation to the background noise present in the transducer output.

Since the Box-Jenkins model is a linear structure, the rational functions B/F and C/D could be independently parameterized (Ljung, 1999).

The order of polynomials was estimated using the Akaike Information Criterion – AIC (Akaike, 1981).

Two signal enhancers were calculated for each gas concentration transducer: one using a modified normalized least-mean square (NLMS) adaptive finite impulse response (FIR) filtering technique (Diniz, 1997), and the other using the FFT-Wiener technique (Press, 1992).

Adaptive filtering

The filter shown in Figure 1 was simulated in Matlab®, using the Box-Jenkins models previously obtained. The routine which implemented this algorithm is provided in Appendix C. A random noise with the PSD of human signals obtained from Garcia *et al*. (2007) was injected at input $y(n)$ during the training period. A decreasing step-size was used to speed up the convergence of the adaptive filter (see Appendix C). The delay line length (in samples) was adjusted to locate the most significant coefficients of the adaptive FIR filter at the center region of the coefficient vector. The length of the delay and the order of the FIR filter were chosen in order to avoid significant filter coefficients to be truncated. After convergence of the filter, its coefficients were frozen. The resulting FIR filter is an approximation of the optimal causal filter, i.e., the causal filter that minimizes the mean-square error (MSE) between the true signal $y(n)$ and its estimation $\hat{y}(n)$. The FIR filter can be used with true signals obtained with the transducer. For performance evaluation purposes, the MSE between y and the estimate $\hat{y}(n)$ was calculated by injection of a pseudo-random binary sequence (PRBS) in $y(n)$.

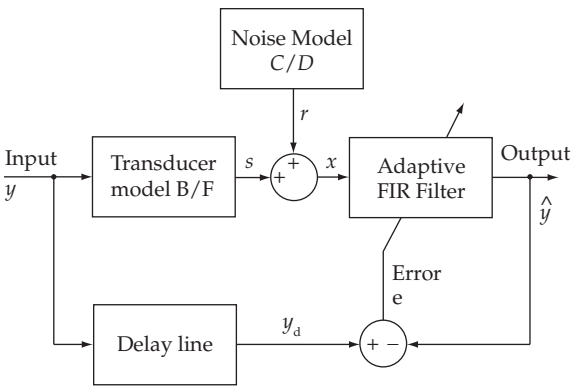

Figure 1. Adaptive filter structure.

The background noise gain k_{cd} of transducer model was reduced 1 to 20 times during the training period. This forced the filter frequency response to have higher gains in frequencies between 3 and 15 Hz due to a better signal-to-noise ratio for $x(n)$. We noticed that with this modification the MSE obtained during the evaluation period was improved and the enhanced signal presented a better step-shape with a PRBS stimulus.

FFT-Wiener filtering

The second technique tested was Wiener filtering via fast Fourier transform (FFT), exactly as described by Press (1992). Let $\mathbf{Y}(f)$ be the FFT of the true respiratory signal at the transducer input. Equation 7 calculates $\hat{\mathbf{Y}}(f)$, i.e., the FFT of the optimal estimate of $\hat{\mathbf{Y}}(f)$.

$$\hat{\mathbf{Y}}(f) = \frac{\mathbf{X}(f) \cdot \Phi(f)}{\mathbf{G}(f)} \tag{7}$$

where $\mathbf{X}(f)$ is the FFT of the signal obtained at the transducer output; $\mathbf{G}(f)$ is the transducer frequency response; and $\Phi(f)$ is given by (8).

$$\Phi(f) = \frac{|\mathbf{S}(f)|^2}{|\mathbf{S}(f)|^2 + |\mathbf{R}(f)|^2} \tag{8}$$

where $\mathbf{R}(f)$ is the FFT of the background noise at the transducer output; and $\mathbf{S}(f) = \mathbf{G}(f) \cdot \mathbf{Y}(f)$.

For calculation of the filter, $\mathbf{Y}(f)$ is obtained from the average human signal PSD evaluated by Garcia *et al.*, and $\mathbf{G}(f)$ and $\mathbf{R}(f)$ are obtained from the transducer model. In this case a non-causal filter was obtained. Therefore, for real-time monitoring (when gas exchange is evaluated simultaneously with the acquisition), this filter was applied dividing the signal $\mathbf{X}(f)$ in frames of 1,024 points (equivalent to 10.24 seconds of acquisition). The FFT of each frame is multiplied by the FFT-Wiener filter. The result is the FFT of the output signal, which could be anti-transformed to obtain the output signal. Each output frame must have its first 256 and last 256 samples ignored because of the border distortion artifacts caused by the FFT, which would introduce error in gas exchange measurements. The next input frame, therefore, must be shifted by 512 samples in relation to the current input frame, in order to recover the whole signal. This procedure allows us to evaluate the acquired signals in real time monitoring, no matter how many frames must be filtered. No window functions should be used for the FFT calculations, since those are useful for frequency estimation, not for filtering, as is our case. A window function such as Hamming (Oppenheim and Schafer,

1999) would increase the MSE of the recovered signal by at least 20%. Appendix D presents the entire routine for the modified FFT-Wiener filter design. The filter performance was evaluated with the same PRBS stimulus used for the adaptive filter.

Again the background noise gain of transducer model was reduced 1 to 20 times during the training period for the same reason as before. The performances of FFT-Wiener filters calculated with and without this noise reduction factor are compared in Results section.

Optimal filters validation

Validation was performed with the setup shown in Figure 2. The principle is the same used in the calibration routine described by Huszczuk *et al*. (1990), with added improvements in the gas injection system and the breath simulation mechanism.

The setup employs a computer-based breathing simulator (Hans Rudolph, 1101), which allows us to control respiratory rate (RR) and tidal volume (V_T). The gas exchange in the simulated airway is obtained from the injection of known flows of CO_2 and N_2 in the system. The injection of CO_2 simulates the real production of CO_2 in human lungs. The injection of both CO_2 and N_2 causes the reduction of O_2 concentration in exhaled air, simulating O_2 consumption by the lungs. The inhaled volume given by this setup is smaller than the real condition, but this does not affect the calculation of $\dot{V}O_2$ and $\dot{V}CO_2$, since the concentration of O_2 and CO_2 in the inhalation phase is the same as the atmospheric concentrations, therefore the contribution to $\dot{V}O_2$ and $\dot{V}CO_2$ will be zero (relative to atmospheric concentrations) during the inhalation phase independently of measured flow.

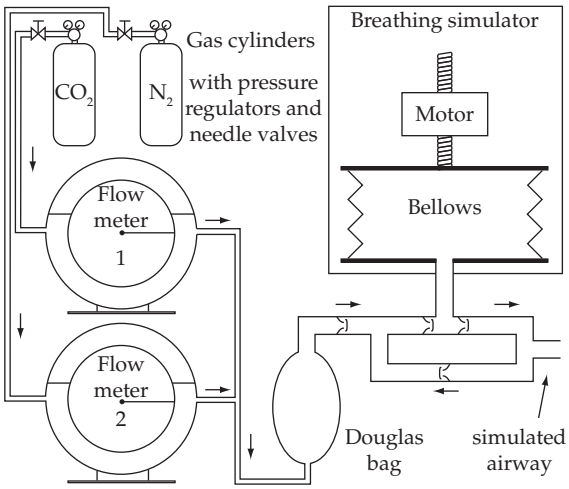

Figure 2. Setup for validation of metabolic measurements. The breathing simulator controls the expiration volume. The increase of CO_2 and decrease of O_2 during expiration is obtained by controlled injection of CO_2 and N_2 in the system. The flow of gas injection is precisely controlled by valve needles and precision flow meters.

The flow meters used were the calibrated instruments (Ritter, TG-3) for CO_2 flow measurement, and (Ritter, TG-50) for N_2 flow measurement. Both gases were injected in a 3-liter Douglas bag before being injected into the simulator. The unidirectional valve setup shown in Figure 2 was made with two two-way valves (Hans Rudolph, 2700B).

The 1101 breathing simulator has the ability to generate from 1 to 99 breaths per minute with an accuracy of 5% in its tidal volume. However, that accuracy did not affect the accuracy of the measured $\dot{V}O_2$ and $\dot{V}CO_2$ in our setup, with the assumption that the inspired and expired volumes given by the simulator were the same. Actually, the accuracy in $\dot{V}O_2$ and $\dot{V}CO_2$ obtained with the setup depended on the accuracy of the flow meters TG-3 and TG-50, which was 0.20%.

The setup can simulate human-shaped flow and gas concentration patterns with configurable RR, V_T, $\dot{V}O_2$ and $\dot{V}CO_2$. Flow and gas concentration signals were acquired for all the transducers, and $\dot{V}O_2$ and $\dot{V}CO_2$ measurements obtained with and without optimal filters were compared with the $\dot{V}O_2$ and $\dot{V}CO_2$ predicted by the setup. Measurement error curves for $\dot{V}O_2$ and $\dot{V}CO_2$ were plotted as a function of RR. The measurement error was calculated as the quotient between the obtained gas exchange measurement and the gas exchange predicted by the setup.

Results

Transducer modeling

For each transducer, average step responses were taken from 8 balloons. The models were evaluated with the algorithm described in Appendix A. Models with orders between 2 and 8 had to be evaluated in order to give the necessary information to enable us to choose the appropriate model order according to the Akaike information criterion. The model parameters for each transducer are shown in Table 1. Figure 3a compares the empirical step response of each transducer with the step response of each respective model obtained.

Design of optimal filters

Once the models were found, optimal filters could be calculated with a modified NLMS adaptive FIR

Table 1. Zeroes and poles of transducers Box-Jenkins models.

PM1111-E (paramagnetic O_2 transducer) model parameters			
B/F ($k_{bf} = 1.3444 \cdot 10^{-2}$)		*C/D* ($k_{cd} = 2.080 \cdot 10^{-3}$)	
Zeroes	Poles	Zero	Pole
$0.82974 \pm 0.27818j$	$0.92015 \pm 0.12087j$	0.40330	–0.22790
0.79620	$0.94518 \pm 4.423 \cdot 10^{-2}j$	-	-
0.64137	-	-	-
Zr733 (galvanic cell O_2 transducer) model parameters			
B/F ($k_{bf} = 8.437 \cdot 10^{-3}$)		*C/D* ($k_{cd} = 6.2733 \cdot 10^{-2}$)	
Zeroes	Poles	Zero	Pole
$0.79478 \pm 0.28454j$	0.94672	0.23710	–0.27620
0.23145	$0.92255 \pm 9.459 \cdot 10^{-2}j$	-	-
S-3A/I (galvanic cell O_2 analyzer) model parameters			
B/F ($k_{bf} = 3.090 \cdot 10^{-3}$)		*C/D* ($k_{cd} = 2.616 \cdot 10^{-3}$)	
Zeroes	Poles	(zero-order noise model)	
0.97039	0.97226	-	-
$0.72365 \pm 0.40655j$	0.91021	-	-
$0.28151 \pm 0.47373j$	$0.85968 \pm 0.10930j$	-	-
-	0.79274	-	-
Ir1507 (infrared CO_2 transducer) model parameters			
B/F ($k_{bf} = 3.142 \cdot 10^{-3}$)		*C/D* ($k_{cd} = 1.997 \cdot 10^{-3}$)	
Zeroes	Poles	Zeroes	Poles
$0.84567 \pm 0.31252j$	0.96510	$-0.14572 \pm 0.51676j$	$0.70541 \pm 0.29132j$
0.51960	$0.89236 \pm 0.16886j$	-	-
-4.620×10^{-2}	0.86251	-	-
CD-3A (infrared CO_2 analyzer) model parameters			
B/F ($k_{bf} = 7.3547 \cdot 10^{-2}$)		*C/D* ($k_{cd} = 4.840 \cdot 10^{-3}$)	
Zeroes	Poles	Zero	Pole
$0.50783 \pm 0.73357j$	0.82900	–0.74261	0.38908
-	0.66397	-	-

Values are non-dimensional.

filter (Appendix C) and the modified FFT-Wiener algorithm (Appendix D). Each FIR filter has between 130 and 300 coefficients and each FFT-Wiener filter has 1,024 complex frequency components. Since we are using an FIR filter to approximately invert an IIR filter, the length of the FIR filter must be large if the exact inverse has a slowly-decaying impulse response. The values were found with the routines shown in Appendices C and D with parameters supplied in Table 1. Figure 3b shows the coefficients of the FIR filter obtained with the adaptive algorithm.

Figure 3c shows a detail of a PBRS stimulus and the transducer model output. Figure 3d compares the PRBS signal recovered by the FIR filter calculated with and without the noise reduction factor during the training period of the filter. Figure 3e compares the PRBS signal recovered by the FFT-Wiener filter calculated with and without this noise reduction factor. The figure shows that the reduction factor has made the signal at the filter to be closer to the PRBS input than the signal at the transducer output. Table 2 shows the MSE between the PRBS stimulus and the signal obtained from the transducer (2nd column); the MSE between the PRBS stimulus and the transducer with FIR filter (3rd column); and the MSE between the PRBS stimulus and the transducer with the modified FFT-Wiener filter (4th column). All output signals in Table 2 were shifted in the time axis in order to obtain the lowest MSE possible.

Validation

Optimal filters for gas concentration transducers were evaluated with the breathing simulation system described before (Figure 2). The percent errors between predicted and computed $\dot{V}O_2$ (for O_2 transducers) or $\dot{V}CO_2$ (for CO_2 transducers) were obtained as a function of RR. A comparison between the errors obtained with and without optimal filters is shown in Figure 4. A summarized analysis of these curves is shown in Table 3. For each transducer, the table gives

Table 2. Mean-square error of recovered PRBS signals.

Transducer	Without enhancer	FIR enhancer	FFT-Wiener enhancer
PM1111-E	$5.22 \cdot 10^{-5}$	$3.75 \cdot 10^{-5}$	$3.05 \cdot 10^{-5}$
Zr733	$6.62 \cdot 10^{-5}$	$3.82 \cdot 10^{-5}$	$3.82 \cdot 10^{-5}$
S-3A/I	$5.60 \cdot 10^{-5}$	$3.21 \cdot 10^{-5}$	$3.20 \cdot 10^{-5}$
Ir1507	$11.35 \cdot 10^{-5}$	$2.59 \cdot 10^{-5}$	$2.59 \cdot 10^{-5}$
CD-3A	$2.55 \cdot 10^{-5}$	$2.22 \cdot 10^{-5}$	$2.20 \cdot 10^{-5}$

Values are non-dimensional. Output signals with and without enhancer filter were time-aligned to the PRBS input to obtain the minimal MSE.

mean percent errors and the error for gas exchange measurements with and without optimal filters. The table shows the dependence on RR in terms of average increasing of percent error in gas exchange measurement as function of increasing RR.

Discussion

The generated models for gas concentration transducers had a simulated step response practically identical to the actual step response measured with the balloon rupture (Figure 3a). This shows that the system identification procedure described in this paper is suitable for the transducers used in metabolic measurements. We noticed the need for models ranging from second order (CD-3A) to fifth order (S-3A/I), which suggests that the lower order filters of previously mentioned studies for dynamic response compensation could be insufficient for these transducers.

The dynamic responses of the transducers are strongly dependent on sample line length, internal diameter and flow rate. The larger the tube the longer the delay and smaller the dynamic range due to gas dispersion along the tubes. The lower the flow rate, the longer the time for the gas to fill the internal chamber of the transducer, which reduces the dynamic range. Therefore, any modification to these parameters will require a new transducer model design.

Comparing (in Table 2) the performance of the modified FFT-Wiener filters with the respective adaptive filters in the reduction of the measurement MSE, we observed that the modified FFT-Wiener filter achieved a better result (lower MSE) than the one obtained with the adaptive FIR filter for the PM1111-E. For the other transducers, the performance of the two filters were equivalent. There are advantages and disadvantages to both techniques. In addition to its better performance, the FFT-Wiener is much simpler to calculate since it is not iterative and the designer does not have to adjust delay, order of the filter, nor step amplitude, just the FFT length. These values are very critical for the convergence of the adaptive filter. On the other hand, the resulting filter must be used in the frequency domain, which makes its implementation a little more complicated in an actual real-time application. Despite its difficult design, the FIR filter resulting from adaptive technique is very simple to implement, since it is a causal moving average filter. However, the designer must consider that the processing demand will be proportional to the length of the FIR filter.

In validation experiments, the accuracy curves have shown that the greater the RR, the greater the underestimation error in the measurement of $\dot{V}O_2$ and $\dot{V}CO_2$. The application of the optimal filters attenuated the RR dependence, and reduced the metabolic measurement error in all cases. The remaining error in gas exchange measurements, observed in Figure 4, even with the use of optimal filters, can be caused by several reasons, such as: a) remaining output error of the adaptive or FFT-Wiener filter; b) small variations in the sampling line flow, causing de-synchronization between flow signal and the gas concentration signals; c) small variations in the sample line pressure, introducing errors in the gas concentration measurements; d) interference of the presence of O_2 in the CO_2 transducer and vice-versa; e) residual errors in the calibration curve of the flow meter; f) residual error caused by small variations in room air humidity. The tendency of underestimation of gas exchange measurements evidenced in Figure 4 and Table 3 is due to a combination of all these sources of errors. A possible solution to overcome the detectable systematic measurement errors in gas exchange is to apply a correction factor (in the value of gas exchange), equal to the inverse of the mean error (shown in Table 3) and consider this factor as a function of RR, as suggests Table 3. This procedure fixes the systematic mean error of the gas exchange measurements.

Table 4 provides a comparison between the presented results and previous studies. Previous research

Table 3. Summary of metabolic measurement errors with and without optimal filters.

Transducer	Without optimal filter		With optimal filter	
	Mean error %	RR influence %Error / breaths/min	Mean error %	RR influence %Error / breaths/min
PM1111-E	-30.0 ± 4.8	-0.39 ± 0.01	-15.0 ± 2.7	-0.20 ± 0.02
Zr733	-22.6 ± 7.0	-0.56 ± 0.03	-7.2 ± 4.0	-0.22 ± 0.05
S-3A/I	-22.0 ± 7.2	-0.58 ± 0.03	-3.6 ± 4.1	-0.25 ± 0.05
Ir1507	-36.8 ± 6.4	-0.52 ± 0.03	-4.6 ± 3.1	0.18 ± 0.04
CD-3A	-12.6 ± 3.7	-0.08 ± 0.06	-2.1 ± 4.5	-0.06 ± 0.07

Dimensions are indicated at each column. For linear regression fitting, consider the mean % error to be the value at 31.0 breaths/min.

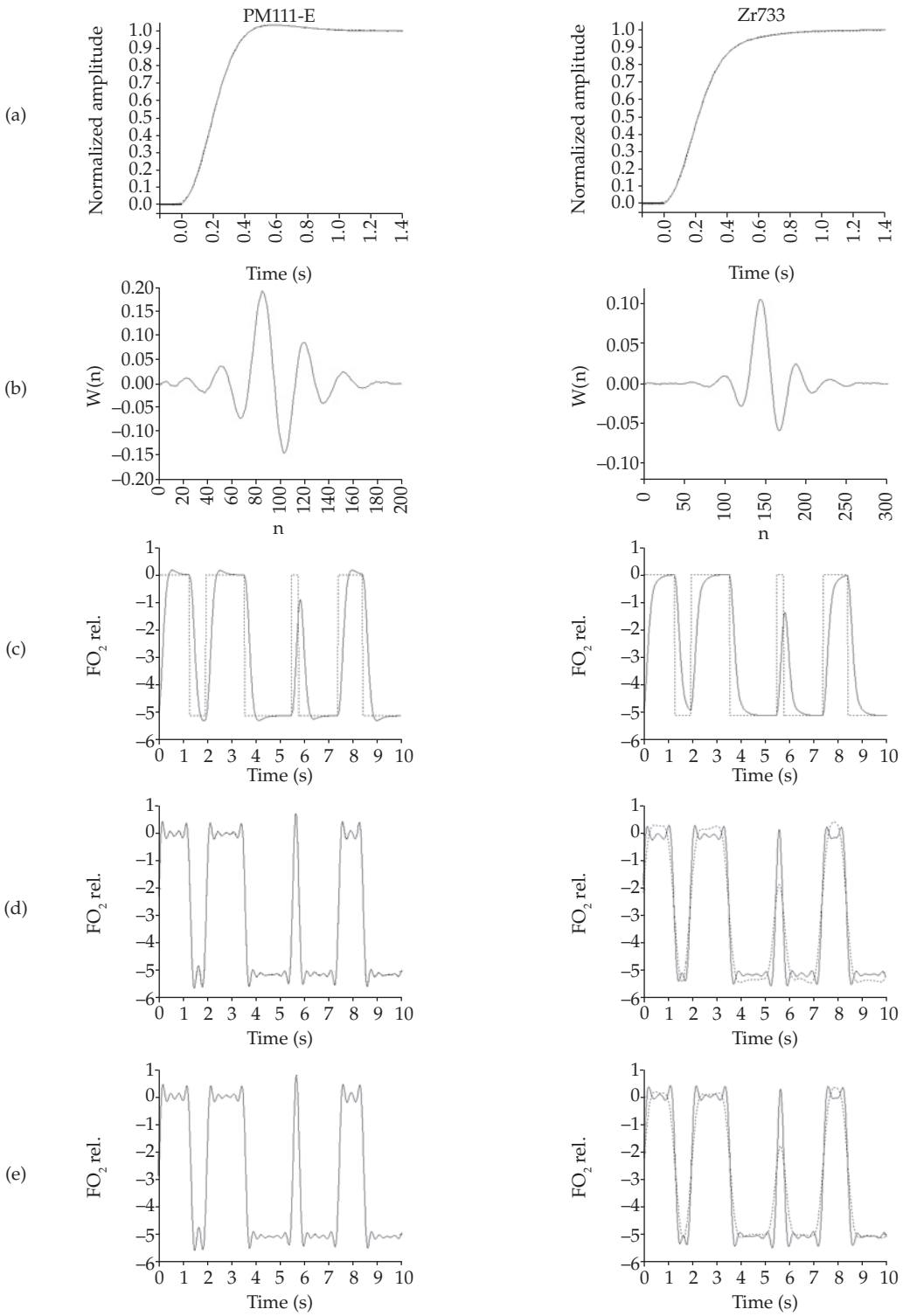

Figure 3. Characteristics of transducer models and respective enhancing filters. a) Comparison between empirical step response (solid line) and the designed model step response (dotted line - almost coincident with solid line, demonstrating the close approximation of the models); b) Coefficients of FIR filter obtained through adaptive algorithm; c) PRBS (dotted line) input and the respective simulated transducer output; d) Recovered PRBS signal with FIR filter with reduction in training noise (solid line) and without reduction in training noise (dotted line); e) Recovered PRBS signal with FFT-Wiener filter with reduction in training noise (solid line) and without reduction in training noise (dotted line). Obs.: signals in rows (d) and (e) are time shifted to compensate the delay caused by the filter, and align the plot with the input PRBS signal.

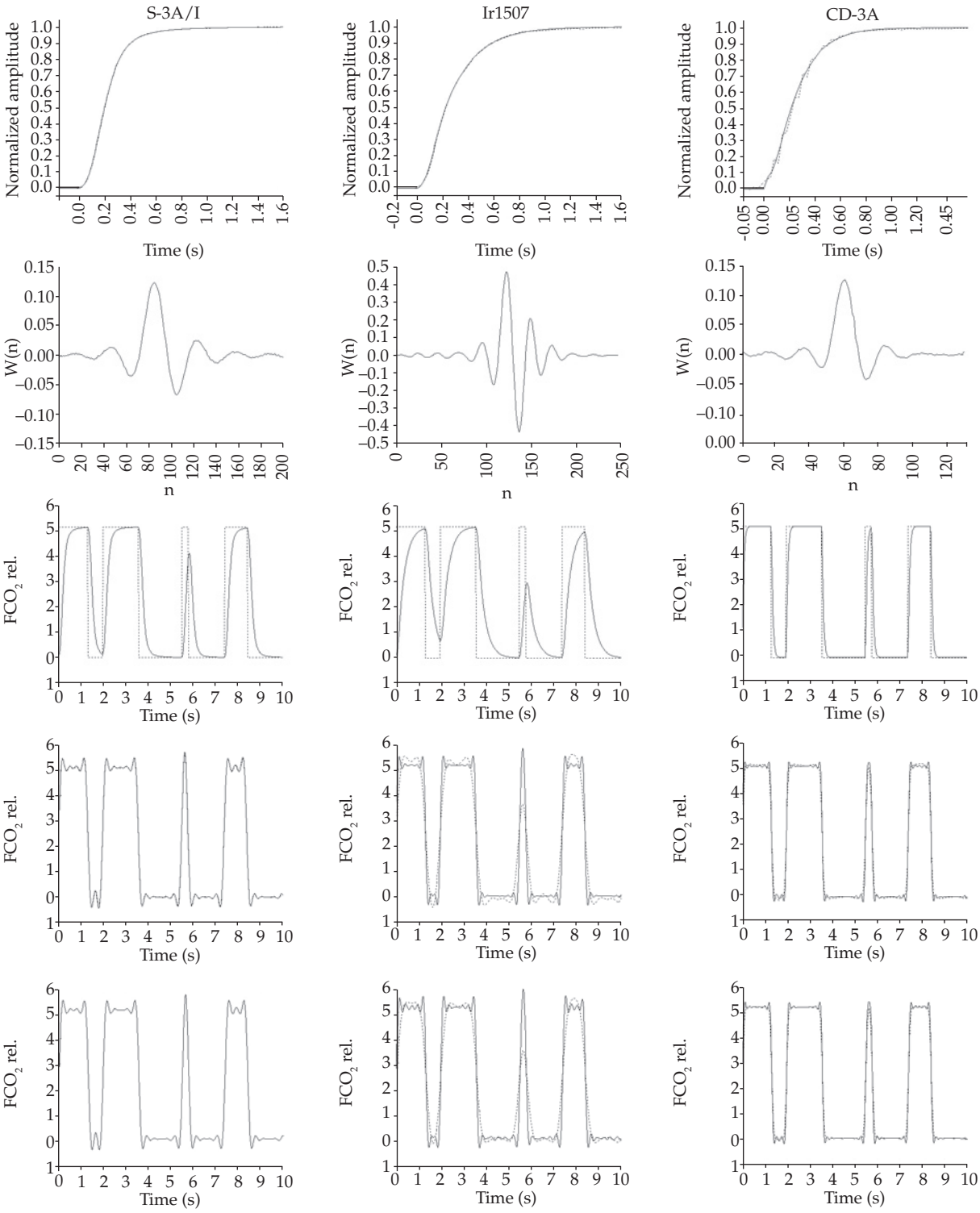

Figure 3. (Cont.)

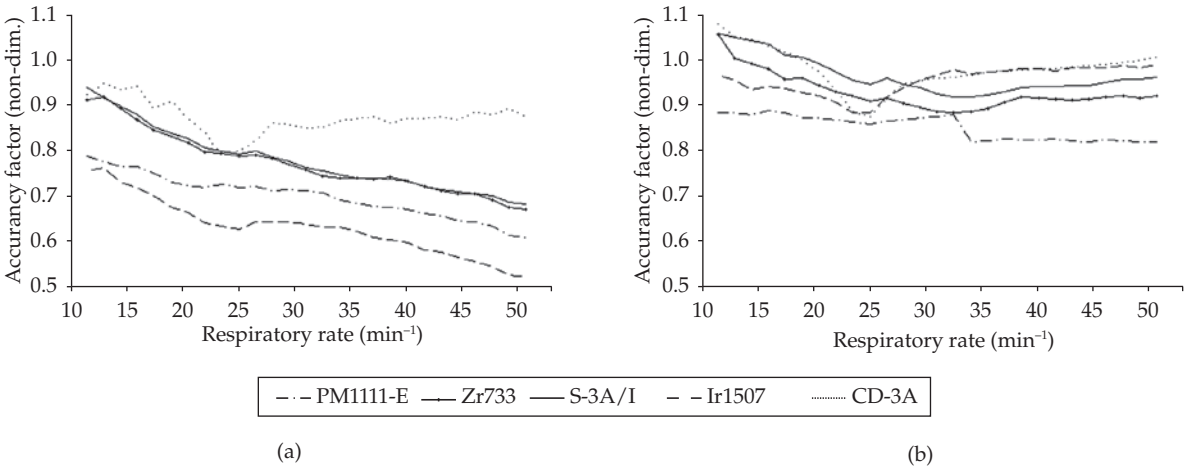

Figure 4. Measurement accuracy factor. a) without optimal filter; b) with optimal filter.

Table 4. Comparison between previous studies.

Authors	Year	Method	Mass spectrometer or Transducers evaluated	Main conclusions	Accuracy obtained in gas exchange measurements %	Precision obtained gas exchange measurements %	RR influence obtained $\frac{\%Error}{breaths/min}$
Arieli and Van Liew	1981	second-order exponential	Vacumetric MMS-100 Perkin-Elmer 1100	"The second-order correction approximates a square output in response to a square input"	not evaluated	not evaluated	not evaluated
Nogushi *et al.*	1982	first-order exponential	Medspect II 7401	"We conclude that to be accurate within ± 5% of the exact value, compensation should be made when time constant exceeds 25 ms"	$\dot{V}O_2$: +3.4 $\dot{V}CO_2$: –3.3	$\dot{V}O_2$: 4.4 $\dot{V}CO_2$: 2.4	not evaluated
Bates *et al.*	1983	Wiener and second-order exponential	Perkin-Elmer MGA-1100	"Wiener filter gave the most accurate corrections in all cases examined"	not evaluated	not evaluated	not evaluated
Shykoff and Swanson	1987	inverse FIR filter	Perkin-Elmer MGA-1100	"Values calculated from data corrupted by a simulated dynamic process return to near the uncorrupted values after correction"	$\dot{V}O_2$ (rest): 0.0 (moderate): –5.0 (heavy): –12.0	not evaluated	evaluated in terms of exercise intensity
Turner and Culbert	1993	third-order IIR model	Medishield MS2	"A third order model with delay fitted to the frequency response predicted the step response very well"	not evaluated	not evaluated	not evaluated
Wong *et al.*	1998	second-order exponential	Datex Ultima	"The algorithm provides an improvement on the relatively slow response times of the clinical gas analyzer"	not evaluated	not evaluated	not evaluated
Farmery and Hahn	2000	four-parameter sigmoid	Datex Ultima	"By inversion of this function, we were able to reduce the rise times for the gases almost fivefold"	not evaluated	not evaluated	not evaluated
Garcia *et al.*	2002	Adaptive filter	S-3A/I	"By the use of this technique, we can significantly reduce the MSE of O_2 concentration signal"	not evaluated	not evaluated	not evaluated
Garcia *et al.*	This paper	Adaptive and FFT-Wiener	PM1111-E Zr733 S-3A/I Ir1507 CD-3A	See "Conclusions" section.	–15.0 –7.2 –3.6 –4.6 –2.1	2.7 4.0 4.1 3.1 4.5	–0.20 –0.22 –0.25 0.18 –0.06

Dimensions are indicated at each column.

groups worked with mass spectrometers due to the fastest step response of such equipment in comparison with galvanic cell transducers. We noticed that Shykoff and Swanson have addressed the issue of accuracy deviation in terms of exercise intensity of the subject. We first characterized this dependence as a function of respiratory rate (RR) and evaluated the reduction of the RR dependence with the use of optimal filters.

The software Matlab® was used in the appendices in order to simplify the routines, since Ljung's System Identification Toolbox contains estimation algorithms implemented for many linear model structures. However, Matlab® is not a requirement and one can choose to implement these algorithms in any other computational environment.

Conclusions

This paper describes practical procedures for optimal filter design for improvement of the frequency response of signals acquired by state-of-the art transducers based on electrochemical cells, infrared absorption and paramagnetic principle. We successfully applied these procedures to metabolic measurements and compared the accuracy of gas exchange measurements with and without the designed filters. Also, we characterized the increase of measurement error with the increase of respiratory rate.

For minimization of gas exchange measurement error we evaluated two techniques: NLMS adaptive filtering and FFT-Wiener filtering. We successfully designed and evaluated an algorithm to apply the FFT-Wiener filter by frames in real-time measurements.

The average gas exchange measurements underestimation was reduced up to 8 times (for Ir1507 the underestimation was reduced from 36.8% to 4.6%). The increasing underestimation of these measurements with the increase of RR was reduced up to 65% (for Ir1507 the RR dependence was reduced from –0.52%/breaths/min. to 0.18 ± 0.04%/breaths/min.), as shown in Table 3.

Comparing the gas exchange accuracy obtained by Nogushi *et al.* (1982) and by Shykoff and Swanson (1987) with those presented in this paper as shown in Table 4 leads to the conclusion that one can achieve an accuracy similar to the accuracy obtained with a mass spectrometer by using galvanic cell and infrared transducers with the use of proper dynamic response compensation.

Acknowledgements

This work was supported by Fundação de Amparo à Pesquisa do Estado de São Paulo - FAPESP under grants 00/08206-7 and 00/08207-3, and by PIBIC/CNPq.

References

Akaike, H. (1981), "Modern development of statistical methods", In: Eykhoff, P., *Trends and progress in system identification*, New York: Pergamon Press.

Arieli, R., Van Liew, H.D. (1981), "Corrections for the response time and delay of mass spectrometers", *Journal of Applied Physiology*, v. 51, n. 6, p. 1417-1422.

ATS/ACCP (2003), "ATS/ACCP statement on cardiopulmonary exercise testing", *American Journal of Respiratory and Critical Care Medicine*, v. 167, n. 2, p. 211-277.

Bates, J.H.T., Prisk, G.K., Tanner, T.E., McKinnon, A.E. (1983), "Correcting for the dynamic response of a respiratory mass spectrometer", *Journal of Applied Physiology*, v. 55, n. 3, p. 1015-1022.

Box, G.E.P., Jenkins, C.W. (1976), *Time series, analysis, forecasting and control*, 2nd ed., San Francisco: Holden-Day.

Diniz, P.S.R. (1997), *Adaptive Filtering: Algorithms and Practical Implementation*, Boston: Kluwer Academic Publishers.

Farmery, A.D., Hahn, C.E.W. (2000), "Response-time enhancement of a clinical gas analyzer facilitates measurement of breath-by-breath gas exchange", *Journal of Applied Physiology*, v. 89, n. 2, p. 581-589.

Garcia, M.A., Cardoso, A.L.R., Silva, A.P., Nascimento, V.H., Moraes, J.C.T.B. (2002), "Enhancement of dynamic response of transducers used in ergospirometry with adaptive and Wiener filtering", In: *Proceedings of the 2nd European Medical and Biological Engineering Conference (EMBEC'02)*, Vienna, v. 3, p. 1462-1463, 04-08 dec.

Garcia, M.A., Nunes, N., Rondon, M.U.P.B., Braga, A.M.F.W., Negrão, C.E., Moraes, J.C.T.B. (2007), "Spectral analysis of respiratory flow and gas concentrations", *in press*.

Huszczuk, A., Whipp, B.J., Wasserman, K. (1990), "A respiratory gas exchange simulator for routine calibration in metabolic studies", *European Respiratory Journal*, v. 3, n. 4, p. 465-468.

Lear, S.A., Brozic, A., Myers, J.N., Ignaszewski, A. (1999) "Exercise stress testing. An overview of current guidelines," *Sports Medicine*, v. 27, n. 5, p. 285-312.

Ljung, L. (1999), *System Identification: theory for the user*, 2nd ed., Englewood Cliffs: Prentice Hall.

Macfarlane, D.J. (2001), "Automated metabolic gas analysis systems: a review", *Sports Medicine*, v. 31, n. 12, p. 841-861.

Madama, V.C. (1993), *Pulmonary Function Testing and Cardiopulmonary Stress Testing*, New York: Delmar Publishers.

McArdle, W.D., Katch, F.I., Katch, V.L. (1996), *Exercise physiology: energy, nutrition and human performance*, 4th ed., Baltimore: Williams & Wilkins.

Myers, J., Madhavan, R. (2001), "Exercise testing with gas exchange analysis", *Cardiology Clinics*, v. 19, n. 3, p. 433-445.

Nogushi, H., Ogushi, Y., Yoshiya, I., Itakura, N., Yamabayashi, H. (1982), "Breath-by-breath $\dot{V}CO_2$ and $\dot{V}O_2$ required compensation for transport delay and dynamic response", *Journal of Applied Physiology*, v. 52, n. 1, p. 79-84.

Oppenheim, A.V., Schafer, R.W. (1999), *Discrete-time signal processing*, 2nd ed., New Jersey: Prentice-Hall.

Press, W.H. (1992), *Numerical recipes in C: the art of scientific computing*, 2nd ed., Cambridge: Cambridge University Press.

Sayed, A.H. (2003), *Fundamentals of adaptive filtering*, Wiley - Interscience.

Shykoff, B.E., Swanson, H.T. (1987), "A model-free method for mass spectrometer response correction", *Journal of Applied Physiology*, v. 63, n. 5, p. 2148-2153.

Singh, V.N. (2001), "The role of gas analysis with exercise testing", *Primary Care*, v. 28, n. 1, p. 159-179.

Turner, M.J., Culbert, S. (1993), "Apparatus to measure the step and frequency responses of gas analysis instruments", *Physiological Measurement*, v. 14, n. 3, p. 317-326.

Weisman, I.M., Zeballos, R.J. (2001), "Clinical exercise testing", *Clinics in Chest Medicine*, v. 22, n. 4, p. 679-701.

White, R.D., Evans, C.H. (2001), "Performing the exercise test", *Primary Care*, v. 28, n. 1, p. 29-53.

Wong, L., Hamilton, R., Palayiwa, E., Hahn, C. (1998), "A real-time algorithm to improve the response time of a clinical multigas analyzer", *Journal of Clinical Monitoring and Computing*, v. 14, n. 6, p. 441-446.

Zeballos, R.J., Weisman, I.M. (1994), "Behind the scenes of cardiopulmonary exercise testing", *Clinics in Chest Medicine*, v. 15, n. 2, p. 193-213.

Appendices

A. Matlab® routine for transducer dynamic response modeling

Note: The empirical step response was averaged from 8 acquisitions, improving resulting step precision, but reducing the transducer background noise. Therefore, the function "bj" was used in this routine to estimate only the IIR model *B/F* in the least squares sense. The disturbance model (*C/D*) was replaced by the one evaluated with the routine described in Appendix B.

```
% Input variables:
% Y=step response acquired from balloon (resampled
%    to 100 Hz) (mean value before transition:
%    forced to zero);
%    (values of Y in % fraction gas)
% pos=position in Y where step response starts;
% amplit=mean non-transitory amplitude between
%    Y levels before and after balloon rupture;
% ord=desired order of polynomials of the model

U=[zeros(pos,1); ones(length(Y)-pos,1)]*amplit;
T=bj(iddata(Y,U,0.01),[ord+1 0 0 ord 0]);
B=T.b;    % B,F=coefficients of polynomials of
F=T.f;    % transducer dynamic response model
          % in direct form II transposed
[Zbf,Pbf,Kbf]=tf2zp(B,F);
          % Zbf,Pbf,Kbf=zeroes, poles and gain of
          % transducer dynamic response model
```

B. Matlab® routine for background noise modeling.

Note: The function "armax" used in this routine with no input signal specification returns an AR-MA model for the given output time series.

```
% Input variables:
% V=transducer signal when input is constant
%    (resampled to 100 Hz);
%    (values of V in % fraction gas)
% ordn= desired order of polynomials of the model
W=V-mean(V);
M=armax(iddata(W,[],length(W)/100),[ordn ordn]);
C=M.c*sqrt(M.NoiseVariance);
D=M.a; % C,D=coefficients of polynomials of
       % transducer background noise model
       % in direct form II transposed
[Zcd,Pcd,Kcd]=tf2zp(C,D);
       % Zcd,Pcd,Kcd=zeroes, poles and gain of
       % transducer background noise model
```

C. Matlab® routine for signal enhancer design with adaptive filtering.

```
% Input variables:
% n=number of iterations;
% m=order of the resulting FIR filter;
% delay=samples delay in adaptive structure;
% ct=constant for better MSE reduction with PRBS;
% Zbf,Pbf,Kbf,Zcd,Pcd,Kcd=zeroes, poles and gains
%    of transducer Box-Jenkins model (see Table 3)
%    (for zero-order noise model: Zcd=[];Pcd=[]);
% Zs,Ps,Ks=zeroes, poles and gain of AR-MA model
of
%    average PSD of input signal (Garcia et al.,
2007)
% U(k)=algorithm step value for iteration k

% values used for each transducer:
%          PM1111E   Zr733  S-3A/I  Ir1507   CD-3A
% n          1.1E6     9E5     5E5   1.9E6     4E5
% m            200     300     200     250     130
% delay        100     160     100     135      65
% ct             1     0.1       1    0.05     0.5
% U(1:k1)      0.5    0.05     0.1     0.1    0.02
% U(k1+1:k2)   0.1    0.01    0.02    0.02    5E-3
% U(k2+1:n)   0.02    2E-3    5E-3    5E-3    1E-3
% k1            6E5     6E5     4E5   1.5E6     2E5
% k2          0.9E6     8E5     3E5   1.7E6     3E5

[B,F]=zp2tf(Zbf,Pbf,Kbf);
[C,D]=zp2tf(Zcd,Pcd,Kcd*ct);
[NumSpec,DenSpec]=zp2tf(Zs,Ps,Ks);
g=max(n+m-1,n+delay); % g=length of random signals
S=filter(NumSpec,DenSpec,randn(1,g)); % S=random
    % signal simulation
S2=filter(B,F,S); % S2=random signal filtered by the
```

```
    % transducer model
R=filter(C,D,randn(1,g))'; % R=random noise model
X=S2'+R; % X=simulated output (signal+noise)
W=zeros(m,1);
WM=zeros(m,1);
for k=1:n
    WA=W;
    XA=X(k+g-n:-1:k+g-n-m+1);
    e=S(k+g-n-delay)-XA'*WA;
    W=WA+XA*(U(k)*e/(XA'*XA));
    if k>n-10000,
        WM=WM+W/10000;
    end
end
WM=WM/sum(WM);
% WM=coefficients of equalizer FIR filter

% Example: filtering a true signal Q with WM:
% (values of Q in % fraction gas)

T=filter(WM,1,Q); % T=Q equalized
```

D. Matlab® routine for signal enhancer design with modified FFT-Wiener filtering.

```
% Input variables:
% Zbf,Pbf,Kbf,Zcd,Pcd,Kcd=zeroes, poles and gains
% of transducer Box-Jenkins model (see Table 3);
% Zs,Ps,Ks=zeroes, poles and gain of AR-MA model of
% verage PSD of input signal (Garcia et al., 2007)
% ct=constant for better MSE reduction with PRBS
% values used for each transducer:
%            PM1111E  Zr733  S-3A/I Ir1507  CD-3A
% ct (FFT-W.)   1       0.1       1   0.05    0.5

[B,F]=zp2tf(Zbf,Pbf,Kbf);
[C,D]=zp2tf(Zcd,Pcd,Kcd*ct);
[NumSpec,DenSpec]=zp2tf(Zs,Ps,Ks);
Rf=freqz(B,F,1024,'whole');
Nf=freqz(C,D,1024,'whole');
Uf=freqz(NumSpec,DenSpec,1024,'whole');
Sf=Rf.*Uf;
Sp=Sf.*conj(Sf);
Np=Nf.*conj(Nf);
Phi=Sp./(Sp+Np);
Ef=Phi./Rf; % Ef=frequency response of equalizer
    % filter

% Example: filtering a true signal X with Ef:
% (values of X in % fraction gas)

sz=length(X);
n=(ceil((sz+512)/512)*512-sz)/2;
p=(n*2+sz)/512-1;
Xe=[zeros(n,1);X;zeros(n,1)];
clear Y
for i=1:p,
    XX=real(ifft(fft(Xe((i-1)*512+1:(i-1)*512 ...
        +1024)).*Ef));
    Y((i-1)*512+1:i*512)=XX(257:768);
end
Y=Y(n-255:sz+n-256)'; % Y=X filtered
```